New Journal of Chemistry

c7nj00739f

We have presented the Graphical Abstract text and image for your article below. This brief summary of your work will appear in the contents pages of the issue in which your article appears.

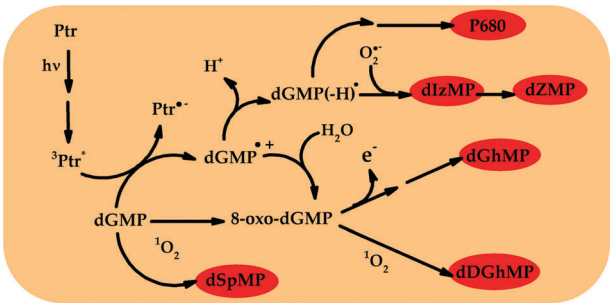

Photosensitized oxidation of 2′-deoxyguanosine 5′-monophosphate: mechanism of the competitive reactions and product characterization

Mariana P. Serrano, Sandra Estébanez Ruiz, Mariana Vignoni, Carolina Lorente, Patricia Vicendo, Esther Oliveros and Andrés H. Thomas*

We have identified five products containing oxidized guanine and another product containing an intact guanine moiety and a modified one.

Q1

Please check this proof carefully. **Our staff will not read it in detail after you have returned it.**

Proof corrections must be returned as a single set of corrections, approved by all co-authors. No further corrections can be made after you have submitted your proof corrections as we will publish your article online as soon as possible after they are received.

Please ensure that:

- The spelling and format of all author names and affiliations are checked carefully. Names will be indexed and cited as shown on the proof, so these must be correct.
- Any funding bodies have been acknowledged appropriately.
- All of the editor's queries are answered.
- Any necessary attachments, such as updated images or ESI files, are provided.

Translation errors between word-processor files and typesetting systems can occur so the whole proof needs to be read. Please pay particular attention to: tables; equations; numerical data; figures and graphics; and references.

Please send your corrections preferably as a copy of the proof PDF with electronic notes attached or alternatively as a list of corrections – do not change the text within the PDF file or send a revised manuscript. Corrections at this stage should be minor and not involve extensive changes.

Please return your **final** corrections, where possible within **48 hours** of receipt, by e-mail to: njc@rsc.org. If you require more time, please notify us by email.

Funder information

Providing accurate funding information will enable us to help you comply with your funders' reporting mandates. Clear acknowledgement of funder support is an important consideration in funding evaluation and can increase your chances of securing funding in the future. We work closely with Crossref to make your research discoverable through the Funding Data search tool (http://search.crossref.org/fundref).

Further information on how to acknowledge your funders can be found on our webpage (http://rsc.li/funding-info).

What is Funding Data?

Funding Data (http://www.crossref.org/fundingdata/) provides a reliable way to track the impact of the work that funders support. We collect funding information from our authors and match this information to funders listed in the Open Funder Registry. Once an article has been matched to its funders, it is discoverable through Crossref's search interface.

PubMed Central

Accurate funder information will also help us identify articles that are mandated to be deposited in PubMed Central (PMC) and deposit these on your behalf.

Providing funder information

We have included the funder information you gave us on submission in the table below. The 'Funder name' shown and their associated 'Funder ID' number is written as listed in the Open Funder Registry. **Please check that the information in the table is correct.** The funder information should match your acknowledgements. This table will not be included in your final PDF but we will share the data with Crossref so that your article can be found *via* the Funding Data search tool.

Funder name	Funder ID	Award/grant/contract number

If a funding organisation you included on submission of your article is not currently listed in the registry it will not appear in the table above. We can only deposit data if funders are already listed in the Open Funder Registry, but we will pass all funding information on to Crossref so that additional funders can be included in future.

Researcher information

If any authors have ORCID or ResearcherID details that are not listed below, please provide these with your proof corrections. Please check that the ORCID and ResearcherID details listed below have been assigned to the correct author. Please use this space to add your own unique ORCID iDs and not another researcher's, as errors will delay publication.

Please also update your account on our online manuscript submission system to add your ORCID details, which will then be automatically included in all future submissions. See here for step-by-step instructions and more information on author identifiers.

First (given) name(s)	Last (family) name(s)	ResearcherID	ORCID
Mariana P.	Serrano		0000-0002-2476-6794
Sandra	Estébanez Ruiz		
Mariana	Vignoni		
Carolina	Lorente		
Patricia	Vicendo		
Esther	Oliveros		
Andrés H.	Thomas		0000-0002-8054-7799

Queries for the attention of the authors

Journal: **NJC**

Paper: **c7nj00739f**

Title: **Photosensitized oxidation of 2′-deoxyguanosine 5′-monophosphate: mechanism of the competitive reactions and product characterization**

For your information: You can cite this article before you receive notification of the page numbers by using the following format: (authors), New J. Chem., (year), DOI: 10.1039/c7nj00739f.

Editor's queries are marked on your proof like this Q1, Q2, etc. and for your convenience line numbers are indicated like this 5, 10, 15, ...

Please ensure that all queries are answered when returning your proof corrections so that publication of your article is not delayed.

Query reference	Query	Remarks
Q1	Please carefully check the spelling of all author names. This is important for the correct indexing and future citation of your article. No late corrections can be made.	

NJC

PAPER

Photosensitized oxidation of 2′-deoxyguanosine 5′-monophosphate: mechanism of the competitive reactions and product characterization

Cite this: DOI: 10.1039/c7nj00739f

Mariana P. Serrano,[a] Sandra Estébanez Ruiz,[a] Mariana Vignoni,[a] Carolina Lorente,[a] Patricia Vicendo,[b] Esther Oliveros[b] and Andrés H. Thomas*[a]

UV-A radiation (320–400 nm) induces modifications to different biomolecules through photosensitized reactions. Oxidized pterins are efficient photosensitizers that accumulate in the skin affected by vitiligo, and photoinduce the oxidation of guanine in a process initiated by an electron transfer from the nucleobase to the triplet excited state of the photosensitizer. In this work, we have investigated the degradation of 2′-deoxyguanosine 5′-monophosphate (**dGMP**) photosensitized by pterin (**Ptr**), the parent compound of oxidized pterins, in aqueous solutions under UV-A irradiation. We have identified five products containing the oxidized guanine moiety: the deoxyribonucleoside 5′-monophosphate derivatives of imidazolone, dehydroguanidinohydantoin, guanidinohydantoin, oxazolone and spiroiminodihydantoin. An additional product with a much higher molecular weight, denoted **P680**, was also detected. The MS/MS analyses show that this compound contains an intact guanine moiety and a modified one. The dependence of the rate of product formation on experimental conditions was analyzed and a general mechanistic scheme is proposed.

Received 4th March 2017,
Accepted 21st June 2017

DOI: 10.1039/c7nj00739f

rsc.li/njc

Introduction

Electromagnetic radiation induces modifications to different biomolecules and is implicated in the generation of human skin cancers.[1] Most of the solar UV energy incident on Earth surface corresponds to UV-A radiation (320–400 nm), which is not absorbed significantly by DNA and proteins, but acts indirectly by photosensitized reactions driven by both endogenous and exogenous photosensitizers. Epidemiological evidence has shown that exposure of humans to artificial UV-A radiation, now recognized as a class I carcinogen,[2] is a major risk factor for melanoma induction.[3–5] Photosensitization is also important due to several applications in disinfection[6,7] and photodynamic therapy (PDT).[8,9]

Pterins, heterocyclic compounds widespread in biological systems in multiple forms, are present in human epidermis because 5,6,7,8-tetrahydrobiopterin (H_4Bip) is an essential cofactor in the hydroxylation of the aromatic amino acids.[10] Several dihydro and tetrahydropterin derivatives participate in the metabolism of H_4Bip and, hence, are also present in human skin.[11] In vitiligo, a skin disorder characterized by a defective protection against UV radiation due to the acquired loss of constitutional pigmentation,[12] the H_4Bip metabolism is altered[13] and unconjugated oxidized/aromatic pterins accumulate in the affected tissues.

In the late 1990s it was reported that UV-A excitation of pterins induces DNA damage.[14–16] In the context of our studies on the photosensitizing properties of pterins, we have previously demonstrated that pterin (**Ptr**), the parent unsubstituted compound of oxidized pterins (Fig. 1a), and the vitiligo-related pterin derivatives (biopterin, formylpterin and carboxypterin) are able to photoinduce the degradation of purine nucleotides (2′-deoxyguanosine 5′-monophosphate (**dGMP**)[17,18] and 2′-deoxyadenosine 5′-monophosphate (dAMP)[19,20]) in aqueous solutions. We have also demonstrated that pterins under UV-A radiation photosensitize pyrimidine nucleotides,[21] biomembranes[22] and proteins.[23,24]

In the case of **dGMP**, mechanistic analyses[25] established that in **Ptr**-photosensitization two competitive pathways take place: (i) one involves electron transfer (type I mechanism) and (ii) the other oxidation by singlet oxygen ($^1O_2$) (type II mechanism). The former process is initiated by an electron transfer from the nucleotide to the triplet excited state of **Ptr** (^{3}Ptr*) yielding the **Ptr** radical anion (Ptr$^{\bullet-}$) and the nucleotide radical cation (dGMP$^{\bullet+}$) (reaction (1)). The latter species efficiently deprotonates to the corresponding **dGMP** neutral radical (**dGMP**(–H)$^\bullet$) (reaction (2)). These radicals may recombine

[a] Instituto de Investigaciones Fisicoquímicas Teóricas y Aplicadas (INIFTA), Departamento de Química, Facultad de Ciencias Exactas, Universidad Nacional de La Plata (UNLP), CCT La Plata-CONICET. Diagonal 113 y 64, (1900) La Plata, Argentina. E-mail: athomas@inifta.unlp.edu.ar; Fax: +54 221 4254642; Tel: +54 221 4257430 ext. 189

[b] Université Toulouse III (Paul Sabatier-Laboratoire des Interactions Moléculaires et Réactivité Chimique et Photochimique (IMRCP), UMR 5623-CNRS/UPS), 118, route de Narbonne, F-31062, Toulouse cédex 9, France

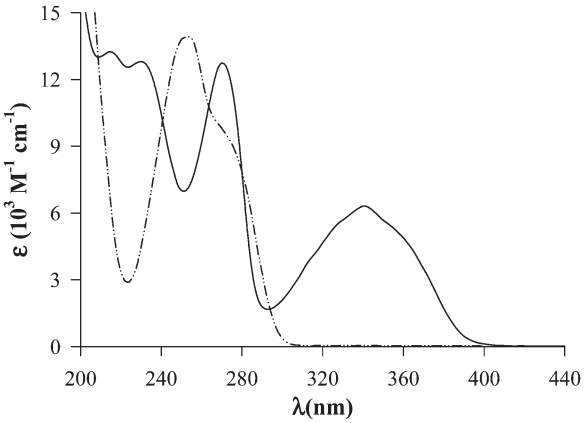

Fig. 1 Absorption spectra in air-equilibrated aqueous solutions at pH 5.5; solid line: **Ptr**; dashed–dotted line: **dGMP**. The spectrum of the mixture is the sum of the two individual absorption spectra.

(reaction (3)), avoiding the formation of products, a predominant reaction under anaerobic conditions. In contrast, in aerated solutions, the electron transfer from $Ptr^{\bullet-}$ to molecular oxygen (O_2) (reaction (4)) prevents radicals recombination (reaction (3)), regenerates **Ptr** and forms superoxide anion ($O_2^{\bullet-}$). The latter may, in turn, disproportionate with its conjugated acid $HO_2^{\bullet}$ to form H_2O_2 (reaction (5)). It has been also reported that $O_2^{\bullet-}$ reacts very fast with guanine radicals according to two parallel pathways: chemical repair with the restoration of the guanine through electron transfer[26,27] and addition.[26,28,29] The former process has been recently demonstrated for **dGMP** (reaction (6)).[25] The oxidation of **dGMP**(–H)$^{\bullet}$ by $O_2^{\bullet-}$ and/or O_2 and/or hydration may lead to different products (reaction (7)).

The type II mechanism is initiated by energy transfer from $^3Ptr^*$ to O_2 leading to the regeneration of **Ptr** and the formation of $^1O_2$ (reaction (8)). The guanine moiety reacts with $^1O_2$ leading to different products[30] (reaction (9)). Several mechanistic and kinetic studies have demonstrated that in the case of the degradation of **dGMP** photosensitized by **Ptr**, the oxidation *via* the type I mechanism is much faster than the oxidation by $^1O_2$.[17,25]

Type I mechanism

$$^3Ptr^* + \mathbf{dGMP} \rightarrow Ptr^{\bullet-} + dGMP^{\bullet+} \quad (1)$$

$$dGMP^{\bullet+} \rightarrow dGMP(-H)^{\bullet+} + H^+ \quad (2)$$

$$Ptr^{\bullet-} + dGMP(-H)^{\bullet} + H^+ \rightarrow Ptr + dGMP \quad (3)$$

$$Ptr^{\bullet-} + O_2 \rightarrow Ptr + O_2^{\bullet-} \quad (4)$$

$$2H^+ + 2O_2^{\bullet-} \rightarrow H_2O_2 + O_2 \quad (5)$$

$$dGMP(-H)^{\bullet} + O_2^{\bullet-} + H^+ \rightarrow \mathbf{dGMP} + O_2 \quad (6)$$

$$dGMP(-H)^{\cdot} \xrightarrow{O_2^{\cdot-}/O_2/H_2O} dGMP(ox) \quad (7)$$

Type II mechanism

$$^3Ptr^* + O_2 \rightarrow \mathbf{Ptr} + {}^1O_2 \quad (8)$$

$$\mathbf{dGMP} + {}^1O_2 \rightarrow dGMP(ox) \quad (9)$$

To the best of our knowledge, the products of the photosensitization of the guanine moiety by compounds present in the skin, such as pterins, have not been studied. Therefore in the work reported here, the products of the photosensitized oxidation of guanine by **Ptr** have been characterized and the mechanisms involved in each case elucidated. In particular, we have focused our work on the events that take place after the formation of the guanine radical cation and lead to different products depending on the conditions (oxygen concentration, solvent, presence of $O_2^{\bullet-}$ scavengers, *etc.*). To achieve these goals we have conducted studies using **Ptr** as a model sensitizer and **dGMP** as a target molecule. The results have been analyzed in the context of previous mechanistic studies[17,18] and compared to those obtained in other compounds containing the guanine moiety, such as nucleosides, oligonucleotides and DNA.

We have carried out the experiments in aqueous solutions containing **Ptr** and **dGMP** at pH 5.5–6.5. Under these conditions UV-A irradiation only produces excitation of the acid form of **Ptr**[25] (pK_a = 7.9[31]) (Fig. 1), which is the predominant species at physiological pH. We chose **Ptr** as the photosensitizer because its photochemical and photophysical properties are well characterized[31] and moreover this compound has been previously used for the photosensitized oxidation of **dGMP** (*vide supra*).[17,18]

Experimental section

General

Pterin (**Ptr**) was purchased from Schircks Laboratories (Jona, Switzerland) and used without further purification. Methanol was provided by Mallinckrodt Chemical. 2′-Deoxyguanosine 5′-monophosphate (**dGMP**), formic acid, superoxide dismutase (SOD) from bovine erythrocytes (lyophilized powder, ≥95% biuret, ≥3000 units per mg protein) and other chemicals were provided by Sigma-Aldrich used without further purification.

All the experiments were carried out in aqueous solutions prepared using deionized water further purified in a Milli Q Reagent Water System apparatus. The specific electrical resistance of water was ∼10 MΩ cm. The pH measurements were performed with a pH-meter sensION + pH31 GLP combined with a pH electrode 5010T (Hach). The pH of the aqueous solutions was adjusted by adding very small aliquots (few μL) of concentrated (0.1–2 M) HCl or NaOH solutions using a micropipette.

Aqueous solutions containing a **Ptr** and **dGMP** were irradiated in 1 cm path length quartz cells at room temperature with a Rayonet RPR lamp emitting at 350 nm (bandwidth ∼20 nm) (Southern N. E. Ultraviolet Co.). Experiments with air-equilibrated solutions were performed in open quartz cells without bubbling, whereas oxygen-saturated solutions were obtained by bubbling for 20 min with this gas, previously water saturated (Linde, purity >99.998%).

Analysis of irradiated solutions

UV/vis spectrophotometric analysis. Electronic absorption spectra were recorded on a Shimadzu UV-1800 spectrophotometer.

Quartz cells (optical path length of 1 cm) were used for the measurements. The absorption spectra of the irradiated solutions were measured at regular time intervals.

High-performance liquid chromatography (HPLC). A Prominence equipment from Shimadzu (solvent delivery module LC-20AT, on-line degasser DGU-20A5, communications bus module CBM-20, auto sampler SIL-20A HT, column oven CTO-10AS VP, photodiode array (PDA) detector SPD-M20A and fluorescence (FL) detector RF-20A) was employed for monitoring the photochemical processes. A Synergi Polar-RP column (ether-linked phenyl phase with polar endcapping, 150 × 4.6 mm, 4 μm, Phenomenex) was used for product separation. Solutions containing 3% of methanol and 97% of 25 mM formic acid (pH = 3.2) were used as mobile phase. In some cases, for further analysis, the products were isolated from HPLC runs (preparative HPLC), by collecting the mobile phase after passing through the PDA detector.

Mass spectrometry analysis. The liquid chromatography equipment coupled to mass spectrometry (LC/MS) system was equipped with an UPLC chromatograph (ACQUITY UPLC from Waters), equipped with a UV/vis detector (Acquity TUV), coupled to a quadrupole time-of-flight mass spectrometer (Xevo G2-QTof-MS from Waters) (UPLC-QTof-MS), equipped with an electrospray ionization source (ESI). UPLC analyses were performed using an Acquity UPLC BEH C18 (1.7 μm; 2.1 × 50 mm) column (Waters), and isocratic elution with 25 mM formic acid (pH = 3.2) at a flow rate of 0.2 mL min^{-1}. The mass spectrometer was operated in positive and negative ion modes. For high mass accuracy, the Q-Tof was calibrated using 0.1% phosphoric acid in 50 : 50 MeOH/H_2O (vol/vol). The instrument drift was compensated by applying a lock mass correction. Depending on the experiment, the protonated guanosine (*m*/*z* 284.0995), the protonated base (*m*/*z* 152.0572), or other product ions were used as lock mass. Therefore the samples were injected in the chromatograph, the components were separated and then the mass spectra were recorded for each peak of the corresponding chromatograms. In addition, mass chromatograms, *i.e.* representations of mass spectrometry data as chromatograms (the *x*-axis representing time and the *y*-axis signal intensity), were recorded using different scan ranges.

Fluorescence spectroscopy. Steady-state and time-resolved fluorescence measurements were performed at room temperature using a single-photon-counting equipment FL3 TCSPC-SP (Horiba Jobin Yvon), described elsewhere.[32] To obtain the fluorescence spectra the sample solution in a quartz cell was irradiated with a CW 450W Xenon source through an excitation monochromator and the luminescence, after passing through an emission monochromator, was recorded at 90° with respect to the incident beam using a room-temperature R928P detector. In time-resolved experiments a NanoLED source (maximum at 341 nm) was used for excitation and the emitted photons, after passing through a monochromator, were detected by a TBX-04 detector and counted by a FluoroHub-B module. The fluorescence quantum yields (Φ_F) were determined from the corrected fluorescence spectra using eqn (10):

$$\Phi_F = \Phi_F^R I A^R / I^R A \quad (10)$$

where I is the integrated intensity, A is the absorbance at the excitation wavelength (λ_{exc}) and the superscript R refers to the reference fluorophore. In our experiments quinine bisulfate (Riedel-de Haën, Seelze, Germany) in 0.5 M H_2SO_4 was used as a reference (Φ_F = 0.546[33]). To avoid inner filter effects, the absorbance of the solutions, at the excitation wavelength, was kept below 0.10.

Results and discussion

Liquid chromatography/mass spectrometry analysis of photoproducts

The products of the **Ptr** photosensitized oxidation of **dGMP** have been characterized by liquid chromatography/mass spectrometry (LC/MS), using a UPLC equipment coupled to a mass spectrometer (UPLC-QTof-MS, see Experimental section). The chromatograms of solutions containing **Ptr** and **dGMP**, recorded before irradiation using the UV/vis detector, showed two peaks at retention times (t_r) of 2.4 and 2.6 min (Fig. 2a). Analyzes were performed in both positive and negative ion modes (ESI^+ and

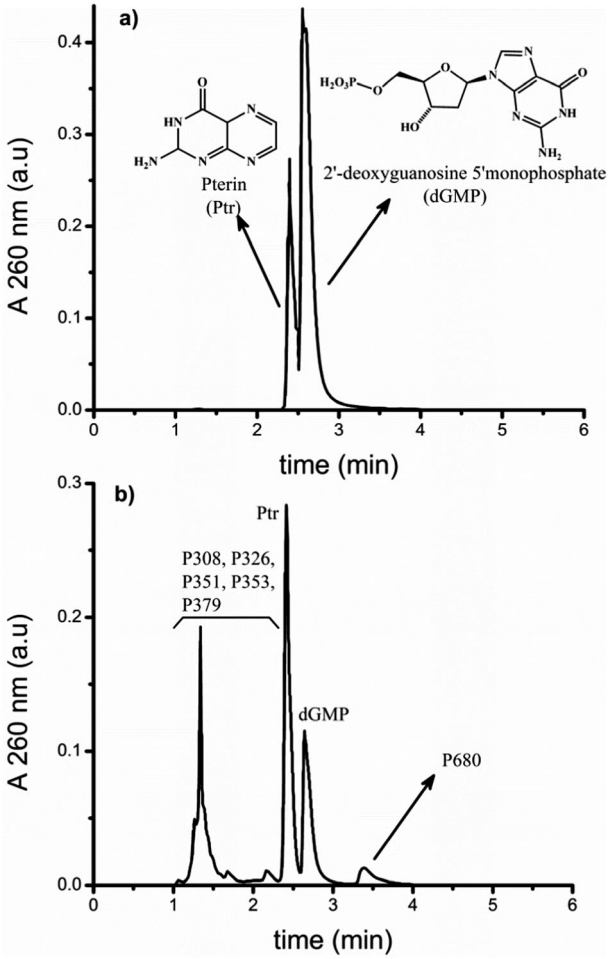

Fig. 2 Chromatograms of air-equilibrated aqueous solutions containing **dGMP** and **Ptr**, recorded using the UV/vis detector (λ_{an} = 260 nm). (a) t_{irr} = 0 min; (b) t_{irr} = 10 min. $[\mathbf{dGMP}]_0$ = 300 μM; $[\mathbf{Ptr}]_0$ = 150 μM, pH = 5.5. In (a) molecular structures of **Ptr** and **dGMP** are depicted.

Table 1 Values of *m/z* recorded for the molecular ions in MS spectra of the reactants and photoproducts

		ESI^+ $[M + H]^+$			ESI^- $[M - H]^-$		
Compound	Elemental composition [M]	Observed *m/z*	Calculated *m/z*	Error (ppm)	Observed *m/z*	Calculated *m/z*	Error (ppm)
Ptr	$C_6H_5N_5O$	164.0565	164.0567	4.5	162.0422	162.0421	3.8
dGMP	$C_{10}H_{14}N_5O_7P$	348.0707	348.0703	0.6	346.0551	346.0558	0.5
P308	$C_8H_{13}N_4O_7P$	309.0607	309.0595	2.2	307.0442	307.0449	0.5
P351	$C_9H_{14}N_5O_8P$	352.0667	352.0653	2.5	350.0501	350.0507	0.2
P353	$C_9H_{16}N_5O_8P$	354.0821	354.0809	1.8	352.0659	352.0664	0.2
P379	$C_{10}H_{14}N_5O_9P$	380.0599	380.0602	2.2	378.0459	378.0456	2.1
P326	$C_8H_{15}N_4O_8P$	327.0721	327.0700	4.7	325.0564	325.0554	4.5
P680	$C_{19}H_{26}N_{10}O_{14}P_2$	681.1197	681.1178	1.9	679.1029	679.1032	0.3

ESI^-, respectively). For the peak at t_r 2.4 min, the signals corresponding to the intact molecular ion of **Ptr** as $[M + H]^+$, $[M + K]^+$ and $[M - H]^-$ species were observed at *m/z* 164.0565, 202.0129 and 162.0422, respectively (M = **Ptr**) (Table 1). For the second peak (t_r = 2.6 min), the signals corresponding to the intact molecular ion of **dGMP** as $[M + H]^+$, $[M + K]^+$ and $[M - H]^-$ species were observed at *m/z* 348.0707, 386.0178 and 346.0551, respectively (M = **dGMP**) (Table 1).

Chromatograms of irradiated solutions, recorded using the PDA detector, showed that the area of the peak corresponding to **dGMP** decreased, indicating that the nucleotide was consumed in the process, in contrast to the photosensitizer as the area of the **Ptr** peak remained constant. These results are in agreement with the behavior reported for the UV-A irradiation of air-equilibrated aqueous solutions containing **Ptr** and **dGMP**.[17]

Besides the peaks corresponding to the reactants, several superimposed peaks with t_r values shorter than that of **dGMP** were detected (Fig. 2b). The mass spectra in ESI^+ corresponding to these chromatographic peaks revealed a set of ions (Table 1), indicating the formation of several photoproducts with the following molecular weights: 308.06, 326.07, 351.07, 353.08 and 379.06 Da. Therefore these products will be named as **P308**, **P326**, P351, **P353** and **P379**, respectively. The mass chromatograms of irradiated solutions recorded for the specific ion masses (Table 1) revealed that each chromatogram presented a unique peak, except for **P353**. In this latter case, at least two isomeric products were formed with the corresponding molecular weight, as the mass chromatogram recorded for the *m/z* value corresponding to **P353** presented two peaks.

An additional chromatographic peak was recorded with a t_r value longer than that of **dGMP** (Fig. 2b). Mass spectra in ESI^+ showed a weak signal at *m/z* 681.1197 (Table 1) with its corresponding Na adduct at *m/z* 703.0257, and several additional peaks at lower *m/z* values (289.0913, 485.1047 and 621.0293). The mass chromatograms recorded for the different ion masses showed peaks with the maxima at the same t_r values and the same shape, suggesting that all the fragments correspond to the same product. For this compound, the resolution was better in ESI^- mode than in ESI^+, and two intense peaks at *m/z* 679.1029 and 339.0528 were observed that correspond to the $[M - H]^-$ and $[M - 2H]^{2-}$ species of the peak at *m/z* 681.1197 observed in ESI^+. Therefore the results suggest that there is at least one product with a t_r higher than **dGMP** with a molecular weight of 680 Da (called **P680**), corresponding to almost twice the molecular weight of the intact nucleotide and that in ESI^+ this product underwent fragmentation very easily. To the best of our knowledge, this is the first time that products derived from photosensitization of nucleotides with so high molecular weights are reported. The analyses of this product performed up-to now in an effort to establish its structure are reported at the end of the Results and discussion section.

Tandem mass spectrometry analyses of photoproducts with t_r values shorter than that of dGMP

The UPLC-QTof-MS equipment was used for tandem mass spectrometry (MS/MS) analysis (Experimental section). The MS/MS spectrum of **dGMP** in the ESI^+ mode (Fig. 3) showed that the loss of the guanine base (G), *via* a 1,2-elimination reaction, yielded the base as a protonated cation ($[G + H]^+$, *m/z* 152.0536). The other observed peaks have already been reported for the fragmentation of compounds bearing the G moiety and correspond to $[G - NH_3 + H]^+$ (*m/z* 135.0265), [G – HNCNH + H]$^+$ (*m/z* 110.0300) and $[C_5H_5O]^+$ (*m/z* 81.0270) (Table 2).[34–36]

Solutions containing **dGMP** (200 μM) and **Ptr** (150 μM) were irradiated for 10 min and the MS/MS spectra of the products listed in Table 1 were recorded. Under these conditions, the peaks of the products **P308**, **P351** and **P353** (Fig. 4) were intense and showed that the typical fragment corresponding to the G moiety at *m/z* 152.0536, present in the MS/MS spectrum of **dGMP** (Fig. 3), was missing. Besides, for all spectra, signals corresponding to chemically modified G were observed: at *m/z* 113.0405 for **P308**, at 156.0524 for **P351** and at 158.0672 for

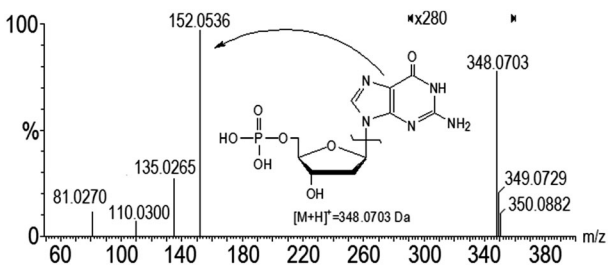

Fig. 3 MS/MS spectrum of **dGMP** recorded in ESI^+ mode and fragmentation of **dGMP** *via* a 1,2-elimination reaction obtained using soft ionization MS methods. Collision energy: 15 eV.

Table 2 Observed and calculated mass/charge ratios, empirical formula and mass errors of compounds and main fragments observed

Fragment [M]	Observed *m*/*z*	Calculated *m*/*z*	Elemental composition $[M + H]^+$	Error (ppm)
dGMP				
G	152.0536	152.0572	$C_5H_6N_5O$	23.9
G-NH_3	135.0265	135.0307	$C_5H_3N_4O$	30.9
G-HNCNH	110.0300	110.0354	$C_4H_4N_3O$	49.4
C_5H_4O	81.0270	81.0340	C_5H_5O	86.9
dIzMP (**P308**)				
Iz	113.0405	113.0458	$C_3H_5N_4O$	51.6
dDGhMP (**P351**)				
DGh	156.0524	156.0521	$C_4H_6N_5O_2$	1.6
dGhMP (**P353**)				
Gh	158.0672	158.0678	$C_4H_8N_5O_2$	3.8
dSpMP (**P379**)				
Sp	184.0448	184.0465	$C_5H_6N_5O_3$	12.3
dZMP (**P326**)				
dZMP–CO_2	283.0796	283.0802	$C_7H_{16}N_4O_6P$	4.1
Z–CO_2	87.0623	87.0671	$C_2H_7N_4$	54.2

P353 (Fig. 4 and Table 2). Taking into account previous analysis reported for the oxidation of G derivatives,[37] these fragments can be assigned to 2,5-diamine imidazolone or simply imidazolone (Iz), dehydroguanidinohydantoin (DGh) and guanidinohydantoin (Gh), respectively (Table 2). Therefore, as expected, the oxidation took place on the G moiety and the detected products can be identified as the corresponding deoxyribonuleoside 5′-monophosphates containing the oxidized G moiety; *i.e.*, **P308**, **P351** and **P353** are dIzMP, dDGhMP and dGhMP, respectively. The chemical structures of these products are depicted in Fig. 4.

To register suitable MS/MS spectra of the other products, a higher initial concentration of the nucleotide (800 μM) and a longer irradiation time (60 min) were needed. In the MS/MS spectra of **P326** and **P379** (Fig. 5), it can be observed that again the fragment of the base G was missing and new peaks corresponding to the modified G moiety appeared. The product **P326** showed the typical fragmentation pattern of compounds bearing 2,2,4-triamino-2*H*-oxazol-5-one or simply oxazolone (Z),[38] with a fragment due to the loss of CO_2 at *m*/*z* 283.0796 and another at *m*/*z* 87.0623 (Fig. 5a and Table 2). The MS/MS spectrum of product **P379**, in turn, presented a peak corresponding to spiroiminodihydantoin (Sp) at *m*/*z* 184.0448[38] (Fig. 5b and Table 2). Consequently, **P326** and **P379** are also products containing the oxidized G moiety, and may be identified as the deoxyribonuleoside 5′-monophosphates derivatives of Z and Sp and will be denoted as dZMP and dSpMP, respectively.

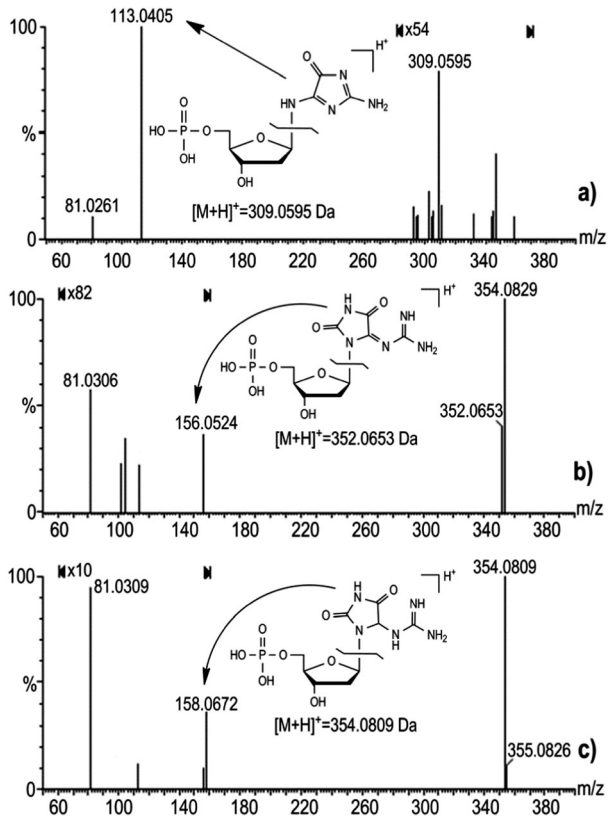

Fig. 4 MS/MS spectra recorded in ESI^+ mode of the products (a) **P308** (dIzMP), (b) **P351** (dDGhMP) and (c) **P353** (dGhMP) formed by **Ptr** photosensitization of **dGMP** in the presence of O_2. Collision energy: (a) 15 eV, (b) 9 eV, (c) 6 eV. The chemical structures of the photoproducts are depicted. $[\mathbf{dGMP}]_0$ = 200 μM, [**Ptr**] = 150 μM, irradiation time = 10 min.

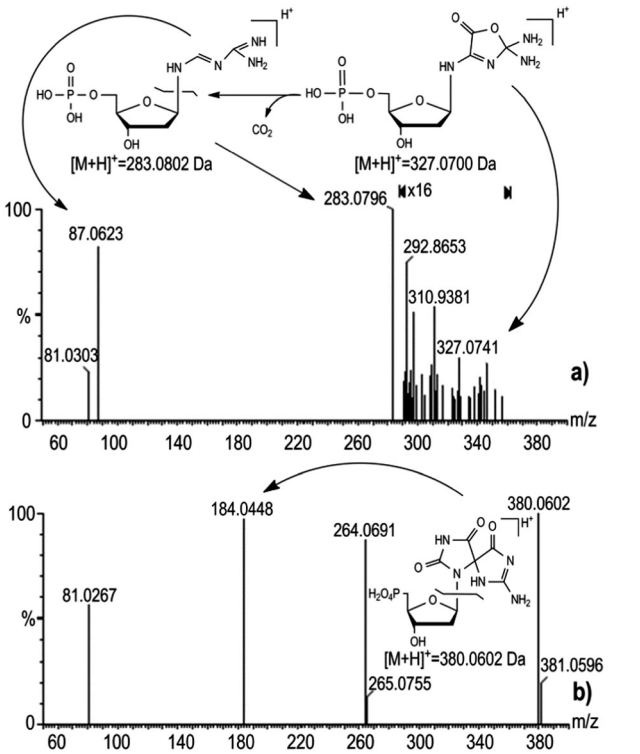

Fig. 5 MS/MS spectra recorded in ESI^+ mode of the products (a) **P326** (dZMP) and (b) **P379** (dSpMP), formed by **Ptr** photosensitization of **dGMP** in the presence of O_2. Collision energy: 15 eV. The chemical structures of the photoproducts are depicted. $[\mathbf{dGMP}]_0$ = 800 μM, [**Ptr**] = 150 μM, irradiation time = 60 min.

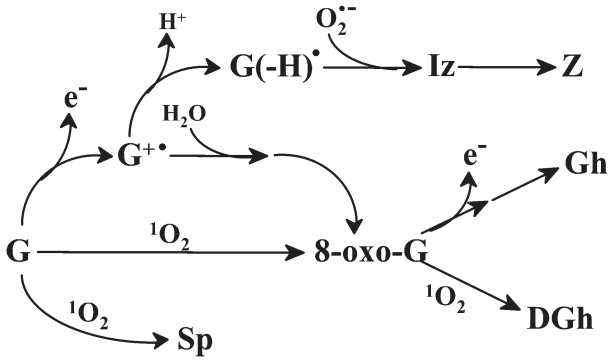

Scheme 1 Photosensitized oxidation of guanine (G) *via* type I (electron transfer) and type II (oxidation by $^1O_2$) mechanisms (8-oxo-G: 8-oxo-7,8-dihydroguanine, Iz: imidazolone, Z: oxazolone, Gh: guanidinohydantoin, DGh: dehydroguanidinohydantoin, Sp: spiroiminodihydantoin).

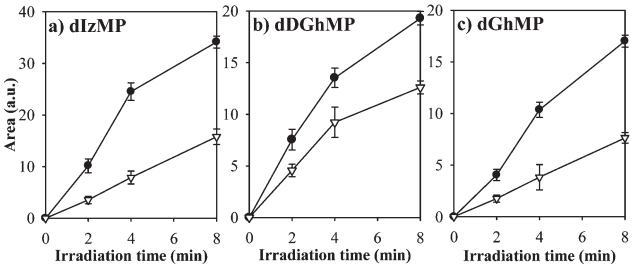

Fig. 6 UPLC-QTof-MS analysis of irradiated solutions containing **dGMP** (300 μM) and **Ptr** (150 μM). Area of the peaks of (a) dIzMP, (b) dDGhMP and (c) dGhMP extracted from mass chromatograms recorded for the corresponding specific masses (chemical structures in Fig. 4). Experiments performed in air-equilibrated solutions (●) and in O_2-saturated (▽).

Although, to the best of our knowledge, no analysis of products of photosensitization of free **dGMP** has been reported, these five compounds correspond to well documented oxidation products of G in different substrates (*e.g.* nucleosides, oligonucleotides, simple and double stranded DNA). The compounds Gh and DGh are products of type I and type II photosensitized oxidation of 8-oxo-7,8-dihydroguanine (8-oxo-G), respectively (Scheme 1).[39–41] This latter compound is formed from G *via* both mechanisms. The corresponding nucleotide 8-oxo-**dGMP** has a molecular weight of 363 Da and was not detected in our system. However, this fact is not surprising since 8-oxo-G is much more reactive than G itself.[42,43] Iz is formed by reaction of the G neutral radical (G(–H)$^\bullet$) with the superoxide anion ($O_2^{\bullet-}$) (Scheme 1).[44] Iz, in turn, yields Z.[26] Finally, oxidation of G by a type II mechanism leads to Sp[45] (Scheme 1).

Dependence of the rate of product formation on experimental conditions

Air/O_2. Consumption of **dGMP** by photosensitization with **Ptr** is faster in air-equilibrated solutions than in O_2-saturated solutions.[17,25] This behavior, observed for the photosensitization of other substrates,[21,46,47] was explained as follows: quenching of triplet excited state of **Ptr** (^{3}Ptr*) (reaction (8)) prevents the electron transfer from the nucleotide to ^{3}Ptr* (reaction (1)), which is the predominant pathway in air-equilibrated solutions. Thus the consumption of **dGMP** due to oxidation by $^1O_2$ is much slower than that initiated by electron transfer. Therefore, although a high O_2 concentration increases the production of $^1O_2$, the net result is a decrease in the rate of **dGMP** consumption. As a consequence, all the products arising from the type I mechanism should be produced at a slower rate in O_2-saturated than in air-equilibrated solutions.

Comparative photolysis experiments were carried out in O_2-saturated and air-equilibrated solutions ([**dGMP**]$_0$ = 300 μM, [**Ptr**] = 150 μM). As expected, the consumption of **dGMP** was slower in O_2-saturated solutions. The mass chromatograms in ESI$^+$ mode for the masses corresponding to the products were recorded at different irradiation times. The peaks corresponding to dIzMP, dDGhMP and dGhMP could be integrated. Although the concentrations of the three products increased with irradiation time under both experimental conditions, the rate of formation was faster in air-equilibrated than in O_2-saturated solutions (Fig. 6). Since the corresponding G oxidation products Iz and Gh are formed *via* a type I mechanism (Scheme 1), these results confirm that the electron transfer pathway, which initiates the degradation of **dGMP**, is inhibited by high O_2 concentrations.

Analysis of the behaviour of dDGhMP is more complex. DGh is formed by oxidation of 8-oxo-G with $^1O_2$ (Scheme 1). As a consequence, the rate of this reaction should increase at high O_2 concentration. However, the reverse behaviour observed (Fig. 6b) can be explained assuming that in the degradation of **dGMP** by **Ptr**, 8-oxo-**dGMP** is mainly formed by a type I photooxidation. Then the quenching of ^{3}Ptr* by O_2, in O_2-saturated solutions, would inhibit the production of 8-oxo-**dGMP** and, as a consequence, the formation of dDGhMP would be also slower, although the steady-state concentration of $^1O_2$ is higher than in air-equilibrated solutions.

D_2O/H_2O. As reported previously,[17,25] the rate of **dGMP** consumption is slightly faster in D_2O than in H_2O, and very far from the extent expected from the differences in $^1O_2$ lifetimes in the two solvents.[48,49] This result suggests that the type II mechanism, albeit taking place, plays a minor role in the overall oxidation of **dGMP** photosensitized by **Ptr**. In our reaction system we have identified dDGhMP and dSpMP that contain the DGh and Sp moieties, respectively, the typical products of the oxidation of G by $^1O_2$ (Scheme 1). To investigate in more detail the pathways that involve $^1O_2$, air-equilibrated solutions containing **Ptr** (150 μM) and **dGMP** (300 μM) in H_2O and D_2O at pH/pD 5.5 were irradiated under otherwise identical conditions. The rates of formation of dIzMP, dGhMP and dDGhMP were practically the same, within experimental error, in D_2O and in H_2O (Fig. 7). These results are in agreement with those presented above and support the hypothesis that the formation of these products is initiated by an electron transfer step.

Even though 8-oxo-**dGMP**, the precursor of dGhMP and dDGhMP, is produced through a type I mechanism, once 8-oxo-**dGMP** is formed, the $^1O_2$-mediated pathway yielding dDGhMP should be strongly enhanced in D_2O. Consequently the ratio dGhMP/dDGhMP should be significantly different in H_2O and D_2O. In contrast, experimental data showed that this ratio was almost the same in both media, suggesting that the

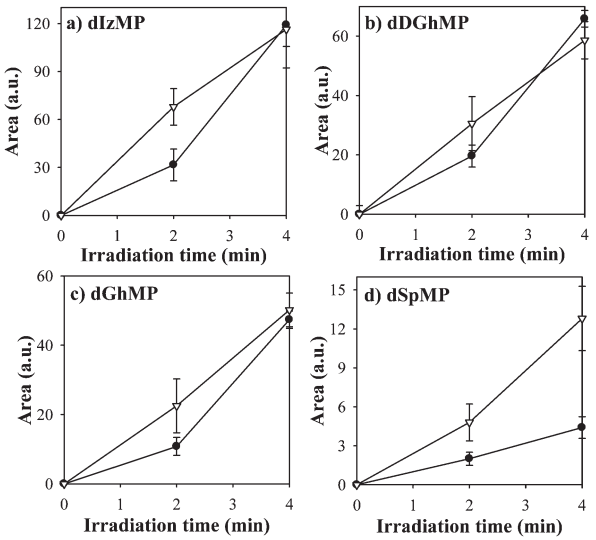

Fig. 7 UPLC-QTof-MS analysis of irradiated air-equilibrated solutions containing **dGMP** (300 μM) and **Ptr** (150 μM). Area of the peaks of (a) dIzMP, (b) dDGhMP, (c) dGhMP and (d) dSpMP extracted from mass chromatograms recorded for the corresponding specific masses (chemical structures in Fig. 4 and 5). Experiments performed in H_2O (●) and in D_2O (▽).

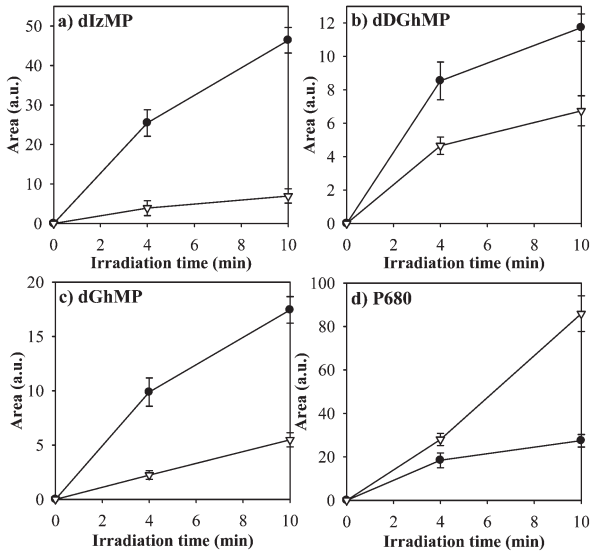

Fig. 8 Analysis of irradiated air-equilibrated aqueous solutions containing **dGMP** (300 μM) and **Ptr** (150 μM). Area of the peaks of (a) dIzMP, (b) dDGhMP, (c) dGhMP extracted from mass chromatograms recorded for the corresponding specific masses (UPLC-QTof-MS). Area of the peak of (d) **P680** extracted from UV-chromatograms recorded at 340 nm (HPLC-PDA). Experiments performed in the absence (●) and in the presence of SOD (50 U ml^{-1}) (▽).

oxidation of 8-oxo-**dGMP** by $^1O_2$ is not the only pathway leading to the formation of dDGhMP.

On the other hand, the rate of SpMP formation was much higher in D_2O than in H_2O (Fig. 7d), which was expected since Sp is a compound reported as a typical product of the oxidation of G by $^1O_2$ (Scheme 1). It is worth mentioning that the increase in the rate of this pathway has a negligible effect on the overall rate of **dGMP** consumption, confirming that the oxidation by $^1O_2$ is a very minor pathway in reactions photosensitized by **Ptr**.

Role of superoxide/SOD. It has been reported that superoxide anion ($O_2^{\bullet-}$) reacts with guanine radicals very fast according to two competitive mechanisms: chemical repair with the restoration of the guanine through electron transfer (reaction (11))[44,50] and addition leading to the predominant formation of 2,5-diamino-4*H*-imidazolone (Scheme 1), dIzMP in our case (reaction (12)).[26–52] In addition, the presence of superoxide dismutase (SOD), an enzyme that catalyzes the conversion of $O_2^{\bullet-}$ into H_2O_2 and O_2,[53] caused a significant increase in the rate of the **dGMP** degradation photosensitized by **Ptr**.[17,25]

This result is due to the decreased efficiency of reaction (11). However, since reaction (12) is also avoided in the presence of SOD, the photosensitized oxidation of **dGMP**, under these conditions, should lead to the increase of the formation of products different from IdZMP (reaction (13)).

$$dGMP(-H)^{\bullet} + O_2^{\bullet-} + H^+ \rightarrow \mathbf{dGMP} + O_2 \quad (11)$$

$$dGMP(-H)^{\bullet} + O_2^{\bullet-} \rightarrow dIzMP \quad (12)$$

$$dGMP^{\bullet+}/dGMP(-H)^{\bullet} \rightarrow dGMP(ox) \quad (13)$$

In order to evaluate the role of $O_2^{\bullet-}$ in the mechanism, air-equilibrated solutions containing **Ptr** (150 μM) and **dGMP** (300 μM) were irradiated in the presence and the absence of SOD (50 U mL^{-1}). As expected, the dIzMP formation in the presence of SOD was much slower than in its absence (Fig. 8a). Surprisingly, although the participation of $O_2^{\bullet-}$ in the production of Gh and DGh has not been reported (Scheme 1), SOD also caused decrease in the rate of formation of the corresponding nucleotides (dDGhMP and dGhMP) (Fig. 8b and c). Therefore, other product(s) must be formed to explain that the **dGMP** consumption is faster, as reported previously.[18]

Although the peak corresponding to the product **P680** could not be integrated to obtain a concentration profile, this product is well separated by HPLC because it appears as the only significant peak with t_r higher than that corresponding to **dGMP**. **P680** could then be analyzed in HPLC-PDA runs and the results showed that **P680** was formed faster in the presence of SOD than in its absence (Fig. 8d). Therefore when the efficiency of reactions (11) and (12) decrease, $dGMP^{\bullet+}/dGMP(-H)^{\bullet}$ participates in other reactions leading to product **P680**. Thus, taking into account the behavior observed in this experiments, we could infer that secondary reactions between $dGMP^{\bullet+}/dGMP(-H)^{\bullet}$ and dGhMP and/or dDGhMP lead to the formation of **P680**.

Analysis of product P680

In this work, we could detect by liquid chromatography and mass spectrometry analyses one product with a t_r value higher than that of **dGMP** and a molecular weight of 680 Da (**P680**), corresponding to almost twice the molecular weight of the intact nucleotide (*vide supra*).

Mass spectrometry analysis. Suitable MS/MS spectra of **P680** in the ESI^- mode could be recorded (Fig. 9) and interpreted

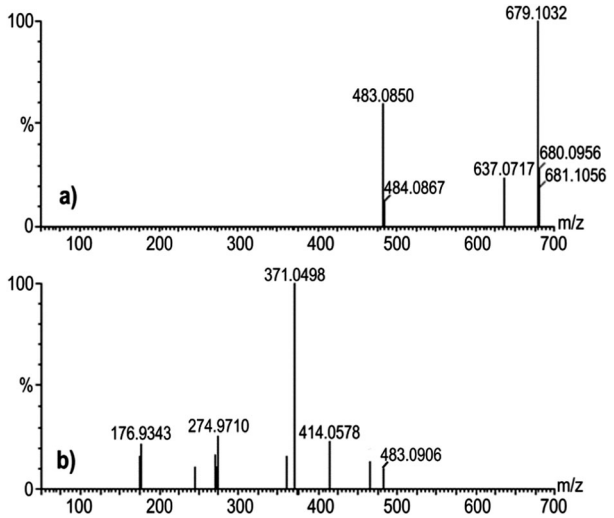

Fig. 9 MS/MS spectra recorded in ESI^- mode of the product **P680** formed by **Ptr** photosensitization of **dGMP** in the presence of O_2. (a) Collision energy: 15 eV, (b) collision energy: 30 eV. $[\mathbf{dGMP}]_0$ = 800 μM, [**Ptr**] = 150 μM, irradiation time = 60 min.

according to a 1,2-elimination that is the typical fragmentation of nucleotides using soft ionization MS methods.[54] At low collision energy, the loss of the 2′-desoxyribose 5′-phosphate leads to a predominant peak at *m/z* 483.0850 (elemental composition $C_{14}H_{16}N_{10}O_8P$, calculated *m/z* 483.0890, error 8.3 ppm) (Fig. 9a). At higher collision energy, among the many fragments observed (Fig. 9b), the ion at *m/z* 176.9343 is a well-known fragment corresponding to the 2′-desoxyribose 5′-phosphate moiety.[54]

On the other hand, MS spectra in ESI^+ mode of **P680** showed a weak signal at *m/z* 681.1197 and peaks at lower *m/z* values (Fig. 10). If a fragmentation *via* a 1,2-elimination is assumed, the peaks at *m/z* 485.1047 and 289.0913 can be assigned to the fragments of the molecular ion (*m/z* 681.1197) corresponding to the loss of one and two 2′-desoxyribose 5′-phosphate, respectively. The former corresponds to the fragment at *m/z* 483.0850 observed in the MS/MS spectra recorded in ESI^- mode (Fig. 9). These results suggest that **P680** consists in two nucleotides linked by the bases. Moreover, the molecular weight of **P680** corresponds to [dGMP + dDGhMP − H_2O] and the fragment at *m/z* 289.0913 corresponds to $[G + DGh - H_2O + H]^+$ (elemental composition $C_9H_9N_{10}O_2$, calculated *m/z* 289.0904, error 1.1 ppm). Therefore, we can infer that **P680** is formed by one molecule of **dGMP** and one molecule of dDGhMP linked by a reaction between the corresponding bases in which a molecule of H_2O is lost. The participation of dDGhMP is also in agreement with the results of the experiments performed in the presence of SOD (Fig. 8).

Due to its low intensity MS/MS spectra in ESI^+ of the molecular ion of **P680** could not be recorded. However, the ions of *m/z* 485.1047 and 289.0913 could be analyzed. The former showed a fragment of *m/z* 289.0878 ($[G + DGh - H_2O + H]^+$) and other peaks correspond to typical fragmentation of G moiety at *m/z* 272.0592 ($[G + DGh - H_2O - NH_3 + H]^+$), *m/z* 247.0643 ($[G + DGh - H_2O - HNCNH + H]^+$), and the ribose fragment at *m/z* 81.0250 ($[C_5H_5O]^+$) (Fig. 11a). The typical fragmentation of G confirmed that, as suggested in the previous paragraph, a G derivative is present in the structure of **P680**. In the MS/MS spectrum of the ion of *m/z* 289.0904, the peak corresponding to the fragment *m/z* 247.0687 ($[G + DGh - H_2O - HNCNH + H]^+$) was also observed (Fig. 11b), in agreement with the previous analysis. Finally, the MS/MS spectrum of ion *m/z* 621.0300 showed a fragment at *m/z* 152.0523 (Fig. 11c), which corresponds to the guanine moiety.

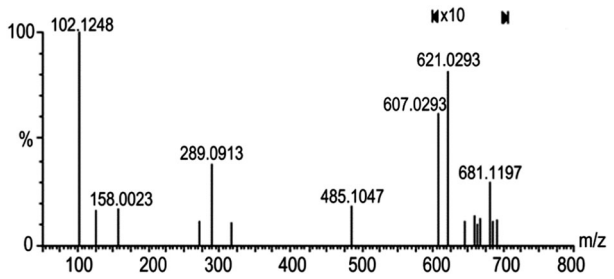

Fig. 10 MS spectrum in ESI^+ mode of the product **P680** formed by **Ptr** photosensitization of **dGMP** in the presence of O_2. Collision energy: 30 eV. $[\mathbf{dGMP}]_0$ = 800 μM, [**Ptr**] = 150 μM, irradiation time = 60 min.

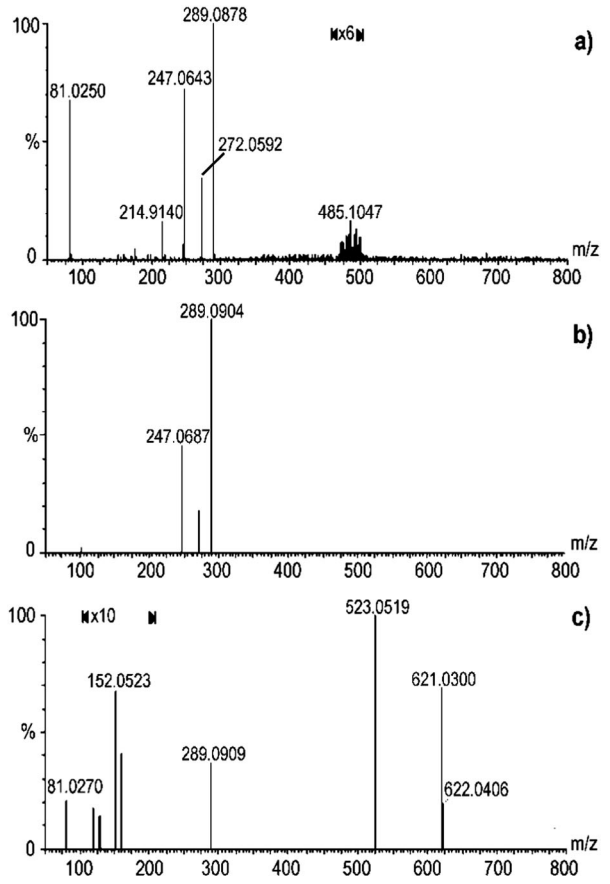

Fig. 11 MS/MS spectra recorded in ESI^+ mode of the product **P680** formed by **Ptr** photosensitization of **dGMP** in the presence of O_2. (a) ion *m/z* 485; (b) ion *m/z* 289, (c) ion *m/z* 621. Collision energy: (a) 25 eV, (b) and (c) 15 eV. $[\mathbf{dGMP}]_0$ = 800 μM, [**Ptr**] = 150 μM, irradiation time = 60 min.

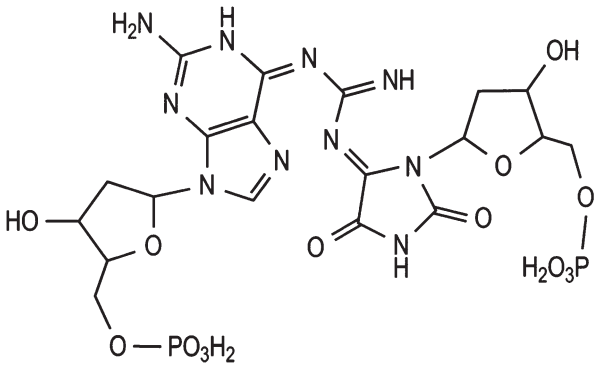

Scheme 2 Proposed chemical structure of product **P680**.

At this stage, it is not possible to propose a definitive chemical structure for the product **P680**. However, taking into account both mass spectrometry and kinetic results in the presence and absence of SOD, we can propose that $dGMP^{\bullet+}$/$dGMP(-H)^{\bullet}$ reacts with dDGhMP to yield an adduct. Although other structures might be hypothesized and, even more, several different products with molecular weight 680 Da might be formed, the chemical structure depicted in Scheme 2 is the one that, in our opinion, better explains most of the fragment observed in mass spectrometry analysis.

Spectroscopic analysis. To obtain additional information about this product, the irradiated solutions were analyzed by HPLC-PDA (Experimental section) and its absorption spectrum was recorded (Fig. 12). It is noteworthy that **P680** presents an absorption band centred at 335 nm that tails into the visible region.

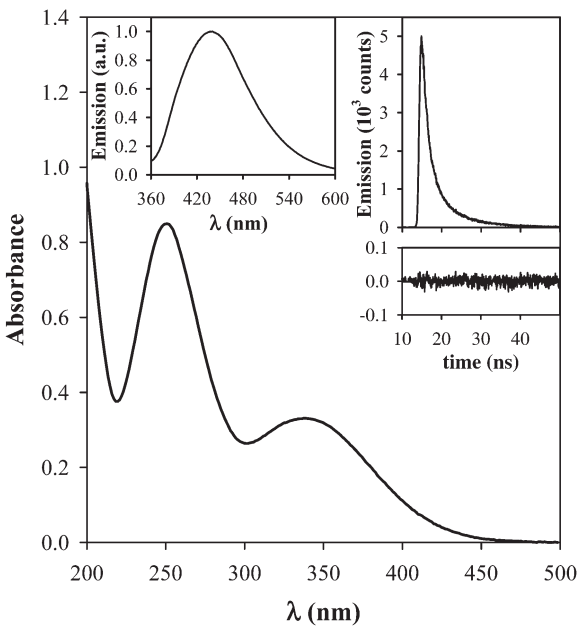

Fig. 12 Spectroscopic features of **P680**. Main graph: absorption spectrum of **P680**. Left inset: Corrected fluorescence spectra (λ_{exc} = 330 nm). Right inset: Emission decay recorded at 440 nm (λ_{exc} = 341 nm), with residual analysis.

To investigate its fluorescence features, the product was isolated from the HPLC runs in aqueous solution and its emission was analyzed (Experimental section). The fluorescence spectrum, upon excitation at 330 nm, shows a band with a maximum at 440 nm (Fig. 12) and the fluorescence quantum yields was determined to be 0.031. Time-resolved experiments were performed by excitation at 341 nm and the emission decays were clearly triexponential with the following components: 0.5 ns, 2.4 ns and 7.9 ns.

Conclusions

The degradation of the 2′-deoxyguanosine 5′-monophosphate (**dGMP**) photosensitized by pterin (**Ptr**), the parent compound of oxidized pterins, in aqueous solution under UV-A irradiation was investigated. We identified five products containing the oxidized guanine moiety: the deoxyribonucleoside 5′-monophosphate derivatives of imidazolone (dIzMP), dehydroguanidinohydantoin (dDGhMP), guanidinohydantoin (dGhMP), oxazolone (dZMP) and spiroiminodihydantoin (dSpMP). Additionally a product denoted **P680** according to its molecular weight was detected. **P680** consists of one molecule of **dGMP** and one molecule of dDGhMP linked by a reaction between the corresponding bases in which a molecule of H_2O is lost. This product presents an absorption band centred at 335 nm that tails into the visible region and fluoresces with a maximum at 440 nm and a fluorescence quantum yield of 0.031. Further studies will be needed to definitively identify **P680** and to investigate the formation of this kind of products in DNA molecules.

The whole of experimental results show that the degradation mechanism of **dGMP** is initiated by an electron transfer from **dGMP** to the triplet excited state of **Ptr** (^{3}Ptr*) yielding the corresponding pair of radicals: $Ptr^{\bullet-}$ and $dGMP^{\bullet+}$. Reaction of the latter in its deprotonated form with superoxide anion leads to dIzMP, which in turn yields dZMP. 8-Oxo-7,8-dihydroguanosine 5′-monophosphate (8-oxo-**dGMP**) is also formed from $dGMP^{\bullet+}$ and then rapidly oxidizes to dDGhMP and dGhMP. The higher molecular weight product **P680** is also formed from $dGMP^{\bullet+}$/$dGMP(-H)^{\bullet}$ and its rate of formation increases when $O_2^{\bullet-}$ is eliminated. This fact indicates that in type I photooxidation of **dGMP**, new products not well characterized up to now are formed upon elimination of $O_2^{\bullet-}$, situation very common in biological systems due to the presence of SOD and other quenchers of this reactive oxygen species. Finally, dSpMP, the only product arising from the oxidation of **dGMP** by $^1O_2$, is a minor product of the **dGMP** photosensitized degradation under our experimental conditions.

Acknowledgements

The present work was partially supported by Consejo Nacional de Investigaciones Científicas y Técnicas (CONICET-Grant PIP 112-200901-00425), Agencia de Promoción Científica y Tecnológica (ANPCyT-Grant PICT-2012–0508), Universidad Nacional de La Plata (UNLP-Grant X712). The authors thank the Centre National de la Recherche Scientifique (CNRS) and CONICET for

supporting their collaboration through a Programme de Coopération Scientifique (CONICET-CNRS/PICS No. 05920). M. P. S. thanks CONICET for her doctoral research fellowship. C. L., M. V. and A. H. T. are research members of CONICET. P. V. and E. O. are research members of CNRS. The authors also thank Nathalie Martins-Froment of the Service Commun de Spectrométrie de Masse (FR2599), Université de Toulouse III (Paul Sabatier) for their valuable help with the mass spectrometry measurements.

References

1 Y. Matsumura and H. N. Ananthaswamy, *Toxicol. Appl. Pharmacol.*, 2004, **195**, 298–308.
2 F. El Ghissassi, R. Baan, K. Straif, Y. Grosse, B. Secretan, V. Bouvard, L. Benbrahim-Tallaa, N. Guha, C. Freeman, L. Galichet and V. Cogliano, *Lancet Oncol.*, 2009, **10**, 751–752.
3 T. B. H. Buckel, A. M. Goldstein, M. C. Fraser, B. Rogers and M. A. Tucker, *Arch. Dermatol.*, 2006, **142**, 485–488.
4 W. Ting, K. Schultz, N. N. Cac, M. Peterson and H. W. Walling, *Int. J. Dermatol.*, 2007, **46**, 1253–1257.
5 J. Moan, A. C. Porojnicu and A. Dahiback, *Adv. Exp. Med. Biol.*, 2008, **624**, 104–116.
6 F. Manjón, L. Villén, D. García-Fresnadillo and G. Orellana, *Environ. Sci. Technol.*, 2008, **42**, 301–307.
7 F. Manjón, D. García-Fresnadillo and G. Orellana, *Photochem. Photobiol. Sci.*, 2009, **8**, 926–932.
8 A. P. Castano, P. Mroz and M. R. Hamblin, *Nat. Rev. Cancer*, 2006, **6**, 535–545.
9 P. Babilas, S. Schreml, M. Landthaler and R.-M. Szeimies, *Photodermatol., Photoimmunol. Photomed.*, 2010, **26**, 118–132.
10 I. Ziegler, *Med. Res. Rev.*, 1990, **10**, 95–114.
11 C. A. Nichol, G. K. Smith and D. S. Duch, *Annu. Rev. Biochem.*, 1985, **54**, 729–764.
12 S. J. Glassman, *Clin. Sci.*, 2011, **120**, 99–120.
13 K. U. Schallreuter, J. Moore, J. M. Wood, W. D. Beazley, E. M. Peters, L. K. Marles, S. C. Behrens-Williams, R. Dummer, N. Blau and B. Thöny, *J. Invest. Dermatol.*, 2001, **116**, 167–174.
14 K. Ito and S. Kawanishi, *Biochemistry*, 1997, **36**, 1774–1781.
15 K. Hirakawa, H. Suzuki, S. Oikawa and S. Kawanishi, *Arch. Biochem. Biophys.*, 2003, **410**, 261–268.
16 T. Offer, B. N. Ames, S. W. Bailey, E. A. Sabens, M. Nozawa and J. E. A. Ayling, *FASEB J.*, 2007, **21**, 2101–2107.
17 G. Petroselli, M. L. Dántola, F. M. Cabrerizo, A. L. Capparelli, C. Lorente, E. Oliveros and A. H. Thomas, *J. Am. Chem. Soc.*, 2008, **130**, 3001–3011.
18 M. P. Serrano, C. Lorente, F. E. M. Vieyra, C. D. Borsarelli and A. H. Thomas, *Phys. Chem. Chem. Phys.*, 2012, **14**, 11657–11665.
19 G. Petroselli, R. Erra-Balsells, F. M. Cabrerizo, C. Lorente, A. L. Capparelli, A. M. Braun, E. Oliveros and A. H. Thomas, *Org. Biomol. Chem.*, 2007, **5**, 2792–2799.
20 M. P. Serrano, C. D. Borsarelli and A. H. Thomas, *Photochem. Photobiol.*, 2013, **89**, 1456–1462.
21 M. P. Serrano, M. Vignoni, C. Lorente, P. Vicendo, E. Oliveros and A. H. Thomas, *Free Radical Biol. Med.*, 2016, **96**, 418–431.
22 A. H. Thomas, A. Catalá and M. Vignoni, *Biochim. Biophys. Acta*, 2016, **1858**, 139–145.
23 M. L. Dántola, B. N. Zurbano and A. H. Thomas, *J. Photochem. Photobiol., B*, 2015, **149**, 172–179.
24 A. H. Thomas, B. N. Zurbano, C. Lorente, J. Santos, E. A. Roman and M. L. Dántola, *J. Photochem. Photobiol., B*, 2014, **141**, 262–268.
25 M. P. Serrano, C. Lorente, C. D. Borsarelli and A. H. Thomas, *ChemPhysChem*, 2015, **16**, 2244–2252.
26 R. Misiaszek, C. Crean, A. Joffe, N. E. Geacintov and V. Shafirovich, *J. Biol. Chem.*, 2004, **279**, 32106–32115.
27 M. Al-Sheikhly, *Radiat. Phys. Chem.*, 1994, **44**, 297–301.
28 J. Cadet, T. Douki and J.-L. Ravanat, *Acc. Chem. Res.*, 2008, **41**, 1075–1083.
29 V. Shafirovich, J. Cadet, D. Gasparutto, A. Dourandin and N. E. Geacintov, *Chem. Res. Toxicol.*, 2001, **14**, 233–241.
30 J.-L. Ravanat, G. R. Martinez, M. H. G. Medeiros, P. Di Mascio and J. Cadet, *Arch. Biochem. Biophys.*, 2004, **423**, 23–30.
31 C. Lorente and A. H. Thomas, *Acc. Chem. Res.*, 2006, **39**, 395–402.
32 M. P. Serrano, M. Vignoni, M. L. Dántola, E. Oliveros, C. Lorente and A. H. Thomas, *Phys. Chem. Chem. Phys.*, 2011, **13**, 7419–7425.
33 S. R. Meech and D. Phillips, *J. Photochem.*, 1983, **23**, 193–217.
34 J.-Y. Salpin, L. MacAleese, F. Chirot and P. Dugourd, *Phys. Chem. Chem. Phys.*, 2014, **16**, 14127–14138.
35 M. Curtis, M. A. Minier, P. Chitranshi, O. D. Sparkman, P. R. Jones and L. Xue, *J. Am. Soc. Mass Spectrom.*, 2010, **21**, 1371–1381.
36 R. Tuytten, F. Lemière, W. van Dongen, E. L. Esmans, E. Witters, W. Herrebout, B. van der Veken, E. Dudley and R. P. Newton, *J. Am. Soc. Mass Spectrom.*, 2005, **16**, 1291–1304.
37 T. Gimisis and C. Cismas, *Eur. J. Org. Chem.*, 2006, 1351–1378.
38 L. Cui, W. Ye, E. G. Prestwich, J. S. Wishnok, K. Taghizadeh, P. C. Dedon and S. R. Tannenbaum, *Chem. Res. Toxicol.*, 2013, **26**, 195–202.
39 J. Cadet, T. Douki, D. Gasparutto and J.-L. Ravanat, *Mutat. Res.*, 2003, **531**, 5–23.
40 S. Raoul and J. Cadet, *J. Am. Chem. Soc.*, 1996, **118**, 1892–1898.
41 W. Luo, J. G. Muller, E. M. Rachlin and C. J. Burrows, *Chem. Res. Toxicol.*, 2001, **14**, 927–938.
42 C. Sheu and C. S. Foote, *J. Am. Chem. Soc.*, 1995, **117**, 6439–6442.
43 R. Bernstein, F. Prat and C. S. Foote, *J. Am. Chem. Soc.*, 1999, **121**, 464–465.
44 R. Misiaszek, C. Crean, A. Joffe, N. E. Geacintov and V. Shafirovich, *J. Biol. Chem.*, 2004, **30**, 32106–32115.

45 J. Cadet, J. L. Ravanat, G. R. Martinez, M. H. Medeiros and P. di Mascio, *Photochem. Photobiol.*, 2006, **82**, 1219–1225.
46 A. H. Thomas, M. P. Serrano, V. Rahal, P. Vicendo, C. Claparols, E. Oliveros and C. Lorente, *Free Radical Biol. Med.*, 2013, **63**, 467–475.
47 C. Castaño, C. Lorente, N. Martins-Froment, E. Oliveros and A. H. Thomas, *Org. Biomol. Chem.*, 2014, **12**, 3877–3886.
48 F. Wilkinson, H. P. Helman and A. B. Ross, *J. Phys. Chem.*, 1995, **24**, 663–677.
49 P. R. Ogilby and C. S. Foote, *J. Am. Chem. Soc.*, 1983, **105**, 3423–3430.
50 M. Al-Sheikhly, *Radiat. Phys. Chem.*, 1994, **44**, 297–301.
51 J. Cadet, T. Douki and J.-L. Ravanat, *Acc. Chem. Res.*, 2008, **41**, 1075–1083.
52 V. Shafirovich, J. Cadet, D. Gasparutto, A. Dourandin and N. E. Geacintov, *Chem. Res. Toxicol.*, 2001, **14**, 233–241.
53 I. Fridovich, *Photochem. Photobiol.*, 1978, **28**, 733–741.
54 S. A. Mcluckey, G. J. Berkel and G. L. Glish, *J. Am. Soc. Mass Spectrom.*, 1992, **3**, 60–70.